EXPERIMENTAL BASED INVESTIGATION OF INDUCTION MOTOR IDENTIFICATION AND CLASSIFICATION

N. GASSARA, W. BAHLOUL
Unité de Commande de Machines et Réseaux de Puissance (CMERP), ENIS
nader_enis@yahoo.fr; wiss.enis@gmail.com

M. CHAABENE, M.B.A KAMOUN
Unité de Commande de Machines et Réseaux de Puissance (CMERP), ENIS
maher.chaabene@cmerp.net; mba.kamoun@enis.rnu.tn

Abstract: *An invariant parameters based modeling and an offline identification of a single cage, double cage and deep bar Induction Motor (IM) are developed. Using steady state electric measurements (voltage, stator current and active power), the IM identification is developed by performing a locked rotor test for different frequencies. The linear Least Squares Technique (LST) and the Genetic Algorithm (GA) are used so as to classify the IM according to its rotor type (single cage, double cage or deep bar). The identification and classification algorithms are validated on four IMs. The accuracy and validity of the algorithms are verified as the NRMSE between measured and simulated speed during starting are less than 2,24%.*

Key words: *Induction motor, Modeling, Offline identification, Classification, Genetic Algorithm.*

1. Introduction

Most of the electric energy needed in industrial application is converted into mechanical one by means of squirrel-cage induction motor (IM) [1]. The analysis and the design of motor drive systems require the IM model parameters. Different rotor types are available: single cage, double cage or deep bar. As the single cage model is not suitable to characterize the dynamic behavior of all IM types [2], many authors adopt the modeling of double cage and deep bar motors by adding rotor branches to the equivalent circuit of the single cage IM using constant parameters [3-10]. Nevertheless, this approach engenders an excess in electrical parameters. Moreover, the identification of these parameters, which uses external measures (current, voltage, speed), leads to an infinity of solutions. Hence, reducing the number of parameters is imposed. The model of invariant parameters is considered as the most efficient method. It resolves the parameter identification using linear regression. The new parameters are called MIVs and define both the dynamic and the steady state behavior of the IM model [11-12]. In literature, a complete survey on the various approaches on offline identification is investigated [13]. Mainly, the linear Least Squares Technique is used [14-16]. The parameters identification is based on the transient measurements (current, voltage, speed). The approach is limited as it requires the measurements derivatives for which a data filtering is necessary. Other authors are interested in the parameters identification by using nonlinear classic methods: Newton-Raphson, Gauss-Newton, Levenberg-Marquardt methods. These methods are based on the standard manufacturer data and/or on the tests. These approaches may lead to local minimum while searching for solution in single direction of the search space [17-20]. The Genetic Algorithm (GA) is known as adequate method that solves complex nonlinear optimization problems. The search of the global minimum is launched in multiple directions which avoids to have a local minimum [21]. Moreover, the GA approach does not include derivates which is not avoidable in presence of noisy measurements. Recently, some authors identify the IM parameters by establishing a GA excited with measurements of transient currents and speed during IM starting. Consequently, accurate speed sensor and fast data acquisition system are required. Although GA necessitates a simulation of the starting of the IM in every step, it does not imply a heavy computation time thanks to the performance of the nowadays computers [23].

In this work, an offline IM identification based upon steady state electric measurements (voltage, stator current and active power) is developed by performing a locked rotor test for different

frequencies. This test supplies data over the slip range variation (from g=0 to g=1) without limitation to the IM's statically stable operating zone. This method allows also a classification of the motor according to rotor type. The present investigation contains four sections. In section two, an IM modeling adopting the MIVs is given. The developed model is generalized for all motor types (single cage, double cage or deep bar rotor). The parameters identification and classification using the linear least squares technique (LST) and the GA are presented in section three. Section four shows the experiment and the validation of the algorithms for four IMs. Finally, a discussion on the obtained results is established. Section five is reserved to the conclusion.

2. MIVs based IM state model

In literature, the IM recognizing based modeling either as single cage, as double cage or as deep bar rotor presents an excess in electrical parameters compared to MIVs model. In fact, when the IM is considered as single cage rotor, its recognizing model necessitates five parameters instead of four in MIVs model. Likewise, the recognizing model of the IM double cage rotor needs eight parameters instead of six in MIVs model [11]. The general equivalent circuit of an IM (single cage, double cage or deep bar rotor) is given by figure 1. In this section, a MIVs state model of the IM is expressed. The core-losses and the magnetic saturation are not taken into consideration.

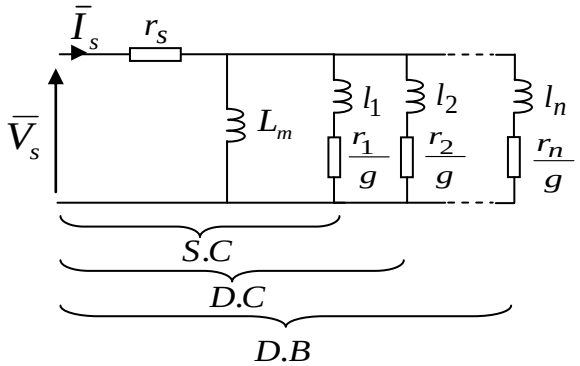

Fig. 1. Equivalent circuit of the IM

S.C: Single cage, D.C: Double cage, D.B: Deep bar

The input impedance of the IM is expressed as:

$$\bar{Z}(\omega,g)=\frac{\sum_{i=0}^{n}\left(j\omega A_{hi}+B_{hi}\right)(j\omega g)^i}{\sum_{i=0}^{n}\frac{B_{hi}}{B_{h0}}(j\omega g)^i} \tag{1}$$

The general MIVs model parameters appear in the numerator and the denominator of the motor's steady-state impedance expression .They are independent of slip (g) and of the supply frequency (ω).The MIVs vector ($MIVs=\left[A_{h0}\ \ A_{h1}\ \ \ldots\ \ A_{hn}\ \ B_{h0}\ \ B_{h1}\ \ \ldots\ \ B_{hn}\right]$) represents the invariant parameters of the IM. Using the equivalent circuit, the MIVs parameters are expressed as:

$$\begin{cases} A_{hj}=L_m\sum\limits_{1\le i_1<\cdots<i_j\le n}\dfrac{l_{i_1}}{r_{i_1}}\dfrac{l_{i_2}}{r_{i_2}}\cdots\dfrac{l_{i_j}}{r_{i_j}} \\ B_{hj}=r_s\left[L_m\sum\limits_{1\le i_1<\cdots<i_j\le n}\left(\dfrac{l_{i_2}l_{i_3}.l_{i_k}+l_{i_1}l_{i_3}.l_{i_k}+\cdots l_{i_1}l_{i_2}.l_{i_{j-1}}}{r_{i_1}r_{i_2}.r_{i_j}}\right)\right. \\ \qquad\left.+\sum\limits_{1\le i_1<\cdots<i_j\le n}\dfrac{l_{i_1}}{r_{i_1}}\dfrac{l_{i_2}}{r_{i_2}}\cdots\dfrac{l_{i_j}}{r_{i_j}}\right] \end{cases} \tag{2}$$

Where j is the rotor branch order $1\le j\le n$. The stator parameters are found for $j=0$ $\left(B_{h0}=r_s;\ A_{h0}=L_s=L_m\right)$.

Reciprocally $(r_1,\ \ldots,\ r_n,\ l_1,\ \ldots,\ l_n)$ are calculated functions of MIVs $\left(A_{hj},B_{hj}\right)$:

$$\begin{cases} r_j=\dfrac{\prod\limits_{\substack{i=1\\ i\ne j}}^{n}\left(a_j-a_i\right)}{\sum\limits_{i=0}^{n-1}(-1)^{n-1-i}\left(\dfrac{B_{h\,n-i}}{A_{h0}B_{h0}}-\dfrac{A_{h\,n-i}}{{A_{h0}}^2}\right)a_j^i} \\ l_j=r_j\,a_j \end{cases} \tag{3}$$

Where a_i are the roots of the polynomial: $A_{h0}a^n-A_{h1}a^{n-1}+\ldots+(-1)^{n-1}A_{h\,n-1}a+(-1)^nA_{hn}=0$

The state model is at first setup according to $\left[r_s,\ L_m,\ r_1,\ \ldots,\ r_n,\ l_1,\ \ldots,\ l_n\right]$ parameters. Using relations (3), the MIVs model is:

$$\begin{cases} \dfrac{dX_e}{dt}=A_eX_e+B_eU_e \\ \dfrac{d\omega_{re}}{dt}=\dfrac{3}{2}\dfrac{p_p^2}{J}A_{h0}\left[i_{sq}\sum\limits_{i=1}^{n}i_{rdi}-i_{sd}\sum\limits_{i=1}^{n}i_{rqi}\right]-\dfrac{p_p}{J}C_R \end{cases} \tag{4}$$

Where:

$X_e=\left[i_{sd}\ \ i_{rd1}\ \ \ldots\ \ i_{rdn}\ \ i_{sq}\ \ i_{rq1}\ \ \ldots\ \ i_{rqn}\right]^T$,

$U_e=\left[v_{sd}\ \ 0\ \ \ldots\ \ 0\ \ v_{sq}\ \ 0\ \ \ldots\ \ 0\right]^T$,

$$A_e = \begin{bmatrix} A_R & -\omega_{re}A_{I1} + A_{I2} \\ \omega_{re}A_{I1} - A_{I2} & A_R \end{bmatrix}, B_e = \begin{bmatrix} B_c & \mathrm{O} \\ \mathrm{O} & B_c \end{bmatrix}$$

$$A_R = -L^{-1}R, \quad A_{I1} = L^{-1}DL, \quad A_{I2} = L^{-1}WL \quad \text{and} \quad B_c = L^{-1}.$$

$$L = \begin{bmatrix} A_{h0} & A_{h0} & \cdots & \cdots & A_{h0} \\ A_{h0} & \dfrac{\prod_{i=2}^{n}(a_1 - a_i)}{\sum_{i=0}^{n-1}(-1)^{n-1-i}\left(\dfrac{B_{h\,n-i}}{A_{h0}B_{h0}} - \dfrac{A_{h\,n-i}}{{A_{h0}}^2}\right)a_1^{i-1}} + A_{h0} & & & \vdots \\ A_{h0} & A_{h0} & \ddots & & \vdots \\ \vdots & \vdots & & \ddots & A_{h0} \\ A_{h0} & A_{h0} & \cdots & A_{h0} & \dfrac{\prod_{i=1}^{n-1}(a_n - a_i)}{\sum_{i=0}^{n-1}(-1)^{n-1-i}\left(\dfrac{B_{h\,n-i}}{A_{h0}B_{h0}} - \dfrac{A_{h\,n-i}}{{A_{h0}}^2}\right)a_n^{i-1}} + A_{h0} \end{bmatrix}$$

$$R = \begin{bmatrix} B_{h0} & 0 & \cdots & 0 \\ 0 & \dfrac{\prod_{i=2}^{n}(a_1 - a_i)}{\sum_{i=0}^{n-1}(-1)^{n-1-i}\left(\dfrac{B_{h\,n-i}}{A_{h0}B_{h0}} - \dfrac{A_{h\,n-i}}{{A_{h0}}^2}\right)a_1^{i}} & & \vdots \\ 0 & 0 & \ddots & \\ \vdots & \vdots & \ddots & 0 \\ 0 & 0 & \cdots & 0 \quad \dfrac{\prod_{i=1}^{n-1}(a_n - a_i)}{\sum_{i=0}^{n-1}(-1)^{n-1-i}\left(\dfrac{B_{h\,n-i}}{A_{h0}B_{h0}} - \dfrac{A_{h\,n-i}}{{A_{h0}}^2}\right)a_n^{i}} \end{bmatrix}$$

$$W = \begin{bmatrix} \omega & 0 & \cdots & & 0 \\ 0 & \omega & & & \vdots \\ 0 & 0 & \ddots & & \\ \vdots & \vdots & & \ddots & 0 \\ 0 & 0 & \cdots & 0 & \omega \end{bmatrix} \text{ and } D = \begin{bmatrix} 0 & 0 & \cdots & & 0 \\ 0 & 1 & & & \vdots \\ 0 & 0 & \ddots & & \\ \vdots & \vdots & & \ddots & 0 \\ 0 & 0 & \cdots & 0 & 1 \end{bmatrix}.$$

3. IM parameters identification

The identification of IM parameters is carried out by means of two methods: the linear least squares technique (LST) which identifies the MIVs by applying Eq.1, and the real coded Genetic Algorithm (GA) which computes the (r_i, l_i) parameters. Since one of the parameters set ((r_i, l_i)or MIVs) is calculated, the other set is deduced thanks to Eq.2 and Eq.3. The parameters A_{h0} and B_{h0}, which correspond respectively to ($(L_s = L_m)$ and r_s) are known. They are measured respectively by no load test and volt-amperemetric experiment. The reduced equivalent circuit of IM is shown by figure 2. Its

parameters R_2 and X_{mot} vary function of the slip (g) and of the supply frequency (ω).

The input impedance of the IM, given by equation 1 is:

$$\overline{Z}(\omega, g) = r_s + R_2 + jX_{mot} \quad (5)$$

Where: $R_2 = \frac{V_s}{I_s}\cos(\varphi) - r_s$, $X_{mot} = \frac{V_s}{I_s}\sin(\varphi)$

and $\cos(\varphi) = \frac{P}{3V_s I_s}$.

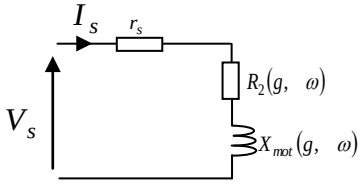

Fig.2.The reduced equivalent circuit of the IM

3.1 LST based identification

Using Eq.5 and Eq.1, the decomposition of the impedance $\overline{Z}(\omega, g)$ in the real and imaginary parts leads to:

$$\sum_{p=0}^{s}(-1)^p \omega^{2p} g^{2p}\left(-\omega A_{h\,2p} + \frac{X_{mot}}{r_s}B_{h\,2p} + \frac{R_2}{r_s}\omega g B_{h\,2p+1}\right) = 0 \quad (6)$$

$$\sum_{p=0}^{s}(-1)^p \omega^{2p} g^{2p}\left(\omega^2 g A_{h\,2p+1} + \frac{R_2}{r_s}B_{h\,2p} - \frac{X_{mot}}{r_s}\omega g B_{h\,2p+1}\right) = 0 \quad (7)$$

Where s is the integer part of $\frac{n}{2}$, n is the number of rotor branches in the IM equivalent circuit . Equations 6 and 7 are valid either n is odd or even. In case n is even $A_{h\,2s+1} = A_{h\,n+1}$ and $B_{h\,2s+1} = B_{h\,n+1}$ are fixed to zero.

The IM parameter identification requires two steps:

Step1: For m values of the slip "g", the variables X_{mot} and R_2 are measured. Accordingly, A_{h2p}, B_{h2p} and B_{h2p+1} are identified by applying the LST algorithm to Eq.6.

Let:

$$\hat{T} = \left[\hat{B}_{h1} \quad \hat{A}_{h2} \quad \hat{B}_{h2} \quad \hat{B}_{h3} \quad \cdots \quad \hat{A}_{h2p} \quad \hat{B}_{h2p} \quad \hat{B}_{h2p+1} \quad \cdots\right]^T$$

$$x_{kp} = -(-1)^p \omega^{2p+1} g(k)^{2p}$$

$$y_{kp} = (-1)^p \omega^{2p} g(k)^{2p} \frac{X_{mot}(k)}{r_s}$$

$$z_{kp} = (-1)^p \omega^{2p+1} g(k)^{2p+1} \frac{R_2(k)}{r_s}$$

Equation 6 becomes:

$$\sum_{p=0}^{s} x_{kp} A_{h\,2p} + y_{kp} B_{h\,2p} + z_{kp} B_{h\,2p+1} = 0 \quad (8)$$

Considering LST approach, for m measurement points, equation 8 is written in matrix form $(1 \le k \le n)$:

$$X\hat{T} = Y$$

Where:

$$X = \begin{bmatrix} z_{10} & x_{11} & y_{11} & z_{k1} & \cdots & x_{1p} & y_{1p} & z_{1p} & \cdots \\ \vdots & \vdots & \vdots & \vdots & & \vdots & \vdots & \vdots & \vdots \\ z_{k0} & x_{k1} & y_{k1} & z_{k1} & \cdots & x_{kp} & y_{kp} & z_{kp} & \cdots \\ \vdots & \vdots & \vdots & \vdots & & \vdots & \vdots & \vdots & \vdots \\ z_{m0} & x_{m1} & y_{m1} & z_{m1} & \cdots & x_{mp} & y_{mp} & z_{mp} & \cdots \end{bmatrix}$$

$$Y = \begin{bmatrix} -x_{10}A_{h0} - y_{10}B_{h0} \\ \vdots \\ -x_{k0}A_{h0} - y_{k0}B_{h0} \\ \vdots \\ -x_{m0}A_{h0} - y_{m0}B_{h0} \end{bmatrix}$$

The parameters A_{h0} and B_{h0} are known, they correspond respectively to L_s and r_s.

As $X\hat{T} = Y$ then $\hat{T} = \left(X^t X\right)^{-1} X^t Y$.

Step2: The obtained values of all $\hat{B}_{hi}$ are used to calculate A_{h2p+1} (Eq.7). This is accomplished by applying the LST again.

Let:

$$\hat{T} = \left[\hat{A}_{h1} \quad \hat{A}_{h3} \quad \hat{A}_{h5} \quad \ldots\right]^T$$

$$x_{kp} = (-1)^p \omega^{2p+2} g(k)^{2p+1}$$

$$y_{kp} = (-1)^p \omega^{2p} g(k)^{2p} \frac{R_2(k)}{r_s}$$

$$z_{kp} = -(-1)^p \omega^{2p+1} g(k)^{2p+1} \frac{X_{mot}(k)}{r_s}$$

$$X=\begin{bmatrix} x_{10} & x_{11} & \cdots & x_{1p} & \cdots \\ \vdots & \vdots & & \vdots & \\ x_{k0} & x_{k1} & \cdots & x_{kp} & \cdots \\ \vdots & \vdots & & \vdots & \\ x_{m0} & x_{m1} & \cdots & x_{mp} & \cdots \end{bmatrix},$$

$$Y=\begin{bmatrix} -y_{10}B_{h0}-z_{10}B_{h1}-y_{11}B_{h2}-z_{11}B_{h3}\cdots-y_{1p}B_{h2p}-z_{1p}B_{h2p+1}\cdots \\ \vdots \\ -y_{k0}B_{h0}-z_{k0}B_{h1}-y_{k1}B_{h2}-z_{k1}B_{h3}\cdots-y_{kp}B_{h2p}-z_{kp}B_{h2p+1}\cdots \\ \vdots \\ -y_{m0}B_{h0}-z_{m0}B_{h1}-y_{m1}B_{h2}-z_{m1}B_{h3}\cdots-y_{mp}B_{h2p}-z_{mp}B_{h2p+1}\cdots \end{bmatrix}$$

Since $X\hat{T}=Y$ then $\hat{T}=\left(X^tX\right)^{-1}X^tY$.

3.2 GA based identification

GAs are stochastic optimization technique that tend to imitate the natural evolution process of species and genetics. These evolving algorithms applied on an optimization problem make develop a set of candidate solutions called population of individuals (or chromosomes). Each individual is characterized by a chain of genes that correspond to the process parameters. To each individual is attributed a function "fitness" that measures the solution's quality it represents, it's often the value of the function to optimize. Then a new population of possible solutions is produced by selecting the parents among the best of the actual generation to make the crosses and the mutations. The new population contains a large proportion of characteristics of the preceding generation best individuals. In this way, from a generation to another, the best genes propagate in the population by combining or exchanging the best features. By favoring the best individuals, the most promoting regions of the research space are explored [21, 22]. (fig.3)

Inequality restrictions on the parameters have been used, $r_1 \le r_2 \le \ldots \le r_n$ and $l_1 \le l_2 \le \ldots \le l_n$. They are included in the algorithm with the following change of variables:

$$\begin{cases} x_1 = r_1 \\ x_2 = r_2 - r_1 \\ x_3 = r_3 - r_2 \\ \vdots \\ x_n = r_n - r_{n-1} \end{cases} \text{ and } \begin{cases} y_1 = l_1 \\ y_2 = l_2 - l_1 \\ y_3 = l_3 - l_2 \\ \vdots \\ y_n = l_n - l_{n-1} \end{cases} \quad (9)$$

With $x_i \ge 0$ and $y_i \ge 0$.

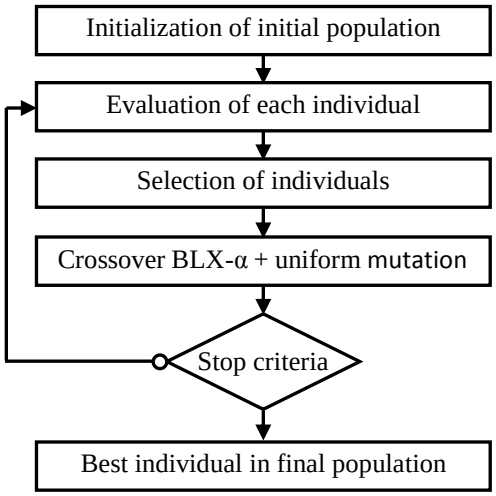

Fig.3. Optimization steps of GA

By applying the GA technique for parameters identification of the IM's, a chromosome (fig.4) contains the $(x_i,\ y_i)$ parameters, where i is the order of rotor branch of the IM model. A real coding is used for this algorithm. The fitness function is the sum of quadratic errors between the measured and the calculated rotor impedances, defined as:

$$Fit=\sum_{k=1}^{m}\left|\bar{Z}'_{re}(k)-\bar{Z}'_{rc}(k)\right|^2 \quad (10)$$

Where "e" is the index of the measured value, "c" corresponds to the index of the calculated value for the evaluated chromosome's parameters and m is the number of measurements for different slips. The expression of the rotor impedance characterized by paralleling n branches (r_i, l_i) is:

$$\bar{Z}'_{rc}(k)=\left[\sum_{i=1}^{n}\frac{1}{j\omega l_i+\dfrac{r_i}{g(k)}}\right]^{-1} \quad (11)$$

$$\bar{Z}'_{re}(k)=\frac{R_2(k)\omega^2L_m^2}{\left(\omega L_m-X_{mot}(k)\right)^2+R_2^2(k)}+j\left(\frac{\omega^2L_m^2\left(\omega L_m-X_{mot}(k)\right)}{\left(\omega L_m-X_{mot}(k)\right)^2+R_2^2(k)}-\omega L_m\right) \quad (12)$$

(r_i, l_i) are deduced from Equation 9 function of x_i and y_i.

The GA algorithm is executed respecting the following conditions:

- The crossover BLX-α is applied with a probability of 0.9.
- The uniform mutation is applied with a mutation probability of 0.01. It's about modifying a

parameter by choosing a new value uniformly at random in the interval defined by the space constraints.

- The individuals' number per population Np is limited to 300.
- The algorithm is stopped when the fitness function (Eq.10) is less than a considered errors fixed to 10^{-5} for seven successive times.

x_1	⋯	x_n	y_1	⋯	y_n

Fig.4. Chromosome representation for the parameters of the IM's rotor branches.

4 Experimental validation

4.1 Experiment description

A test bench has been installed at the National Engineering School, University of Sfax (ENIS) Tunisia. It includes four IMs, an 8KVA alternator, a DC motor and a data acquisition system. The DC motor provides mechanical power to the alternator. The alternator supplies the locked rotor IMs for different frequency. The PC computer in which the algorithm is implemented is connected to an acquisition system which measures stator voltage and stator current. The voltage and current sensors are integrated into the acquisition system. Figure 5a shows the real test bench as for figure 5b gives its synoptic schema.

The IM's identification and classification algorithms require the measurement of R_2 and X_{mot} over the slip range variation ($g \in [0, \ 1]$). Nevertheless, browsing the zone $g \in [g_{C\max}, \ 1]$ cannot be ensured since it represents the instability zone of the IM ($g_{C\max}$ is the slip at the breakdown torque). Therefore, an equivalent test is proposed. This test [24] considers figure 6 where the motor is at locked rotor and supplies by V_{sf} in variable frequency. Instead of varying the load torque to browse the interval of $g \in [0, \ 1]$ in figure 2, it is possible to obtain the same values of R_2 and X_{mot} by performing a locked rotor test for different frequencies $f \in [0, \ 50]$ Hence, the locked-rotor induction motor under test is supplied by a three-phase alternator. This latter allows the adjustment of the frequency and the amplitude of the IM supply. The ratio V_{sf}/f is maintained constant which guaranties a constant magnetic flux. So, the saturation state remains unchanged during the test. The frequency is adjusted by varying the speed of DC motor, while the amplitude is fixed by the excitation voltage of the alternator. Measurements of V_{sf}, I_{sf}, P_{sf} are performed by an acquisition system connected to a PC computer (Fig.5.a,b).

The IM input impedance at locked rotor is (figure 6) :

$$\overline{Z}(\omega, g_{=1}) = r_s + R_{2sf} + jX_{motsf}$$

Where: $R_{2sf} = \frac{V_{sf}}{I_{sf}}\cos(\varphi_{sf}) - r_s$

$$X_{motsf} = \frac{V_{sf}}{I_{sf}}\sin(\varphi_{sf}) \text{ and } \cos(\varphi_{sf}) = \frac{P_{sf}}{3V_{sf}I_{sf}}.$$

Consequently, the IM input impedance for variable speed and fixed frequency is:

$$\overline{Z}(\omega, g) = r_s + R_2 + jX_{mot}$$

First the virtual slip is calculated as: $g = \frac{f}{50}$

Then R_2 and X_{mot} are deduced as [24]:

$$R_2 = \frac{R_{2sf}}{g} \text{ and } X_{mot} = \frac{X_{motsf}}{g}$$

Where $g \in [0, \ 1]$ and $\omega = 100\pi$.

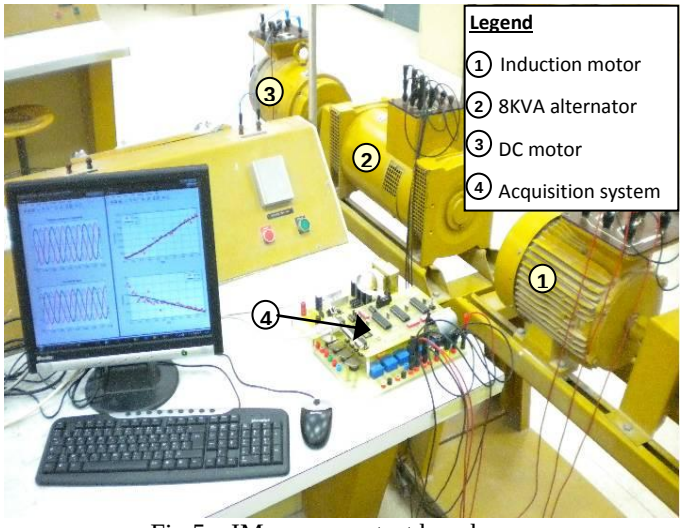

Fig.5.a IM measures test bench.

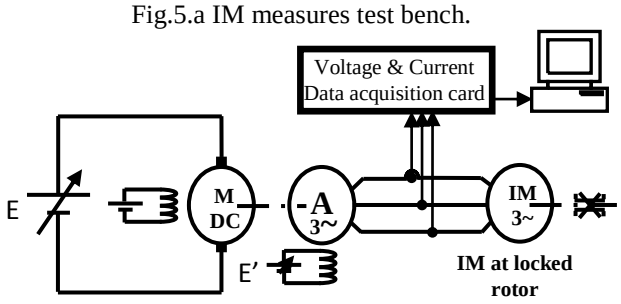

Fig.5.b synoptic schema

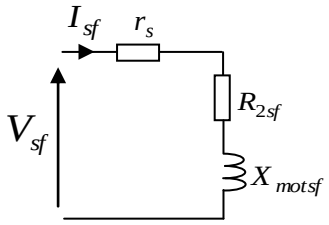

Fig.6. The reduced equivalent circuit of the IM at locked rotor test

4.2 Results and discussion

The developed algorithms are applied to four IMs. Their nominal characteristics are listed in table 1.

Table 1. Name-plate parameters of IMs.

N°	*P(kw)*	*N(rpm)*	*f(Hz)*	*Pp*	*I(A)*	*U(V)*
IM_1	1.1	1390	50	2	4.67	220
IM_2	6	1455	50	2	24	220
IM_3	7.35	725	50	4	28.0	220
IM _4	11	965	50	3	39.2	220

The identification results are presented in tables 2. Identified parameters allow computation of the rotor impedance $\bar{Z}'_{rc}$ using (Eq.11). The comparison between calculated and measured data of $\bar{Z}'_r$ is evaluated by calculating for each IM model the Normalized Root Mean Square Error (*NRMSE%*) defined by (Eq.13), [3]:

$$NRMSE\ (\%) = \frac{\sqrt{\frac{1}{m}\sum_{k=1}^{m}\left(\left|\bar{Z}'_{rc}(k)\right| - \left|\bar{Z}'_{re}(k)\right|\right)^2}}{\frac{1}{m}\sum_{k=1}^{m}\left|\bar{Z}'_{re}(k)\right|} \times 100 \quad (13)$$

Assume the type of rotor is unknown. Then GA and LST algorithms are executed for the three models (n =1, 2, 3 rotor branches). For each case the computed parameters (r_i, l_i) are used to calculate *NRMSE*. The comparison of obtained *NRMSE* classifies the motor in single, double or triple cage (Fig. 7). This procedure is applied to all previously chosen motors (table1).

The parameters of the first branch (r_1, l_1) are accurately identified using only the low slip measurement points.

The rotor impedance is: $\bar{Z}'_r = \frac{R'_r}{g} + jX'_r$

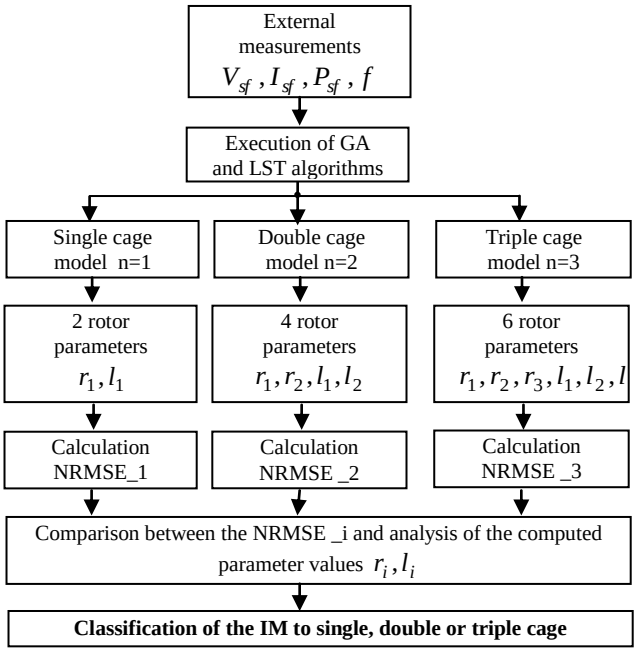

Fig. 7. IM classification procedure

Figures 8, 9, 10 and 11 show measured and calculated R'_r et X'_r in terms of the slip.

Let's consider the IM_1, the LST method provides erroneous parameters (leakage inductance negative) because measurements R'_r et X'_r are too disturbed by measurement noise as is shown in Figure 8. In fact, the measurement of low current leads to a noisy acquisition. In this case GA results become more interesting. The values of *NRMSE* obtained for the models of two and three rotor branches (n = 2, 3) are similar while the *NRMSE* of the single cage model is the highest. Consequently, the double cage model is selected as it is less complicated in use. For the IM_2 motor, the smallest *NRMSE* is obtained with the LST method for the double cage model (n = 2). In this case LST has converged to reasonable results. The shape of the curves R'_r and X'_r are smooth and have no noise. So the assessed IM must be classified as double cage. The identification using LST is very simple since it is reduced to a linear regression according to invariant parameters. However, as it's very sensitive to measurement's errors the measure should be accurate. For IM_3 the smallest *NRMSE* is delivered by the AG method, this latter confirms that the model is of a deep bar rotor with three rotor branches (n = 3). As for the LST method, it gives negative values for the IM parameters which discard this method of classification.

Table 2. Identification results of the IM, LST: Linear least squares technique GA: Genetic algorithm

		r_1 (Ω)	l_1 (H)	r_2 (Ω)	l_2 (H)	r_3 (Ω)	l_3 (H)	NMRSE %
IM_1	LST	2,6670	0,0240					4,89
		2,8607	0,0248	85,254	-0,2737			3,38
		2,8755	0,0273	60,169	0,0770	173,39	-1,295	2,65
	GA	2,6307	0,0238					5,49
		2,7994	0,0277	49,010	0,0277			2,13
		2,7893	0,0274	76,185	0,0274	166,82	0,0548	2,12
IM_2	LST	0,1650	0,0053					9,26
		0,1769	0,0052	5,3089	0,0068			1,34
		0,1764	0,0053	4,7279	0,0065	-70,468	0,0475	1,40
	GA	0,1644	0,0053					10,28
		0,1628	0,0055	4,1352	0,0083			1,89
		0,1622	0,0055	4,4796	0,0108	32,416	0,0164	1,90
IM_3	LST	0,1789	0,0038					5,97
		0,2017	0,0042	2,9735	0,0040			7,12
		0,1960	0,0039	1,1071	0,0034	-1,2332	-0,0067	8,37
	GA	0,1728	0,0038					10,58
		0,1843	0,0045	2,3234	0,0045			2,35
		0,1843	0,0045	2,4244	0,0049	42,763	0,0094	2,02
IM_4	LST	0,1701	0,0028					4,14
		0,1858	0,0031	3,1169	0,0040			2,77
		0,1838	0,0030	2- 4,8i	0,016- 0,006i	2+ 4,8i	0,016+ 0,006i	3,14
	GA	0,1720	0,0029					5,77
		0,1813	0,0032	2,8525	0,0042			2.71
		0,1815	0,0032	2,7580	0,0043	1002,9	0,0435	2,72

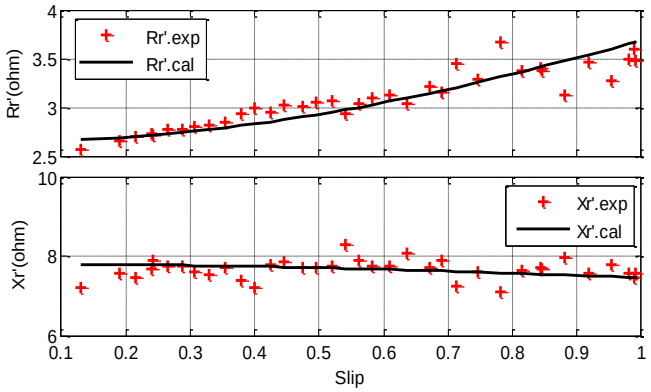

Fig.8. Variation of $R_r^{'}$ and $X_r^{'}$ in terms of slip for IM_1

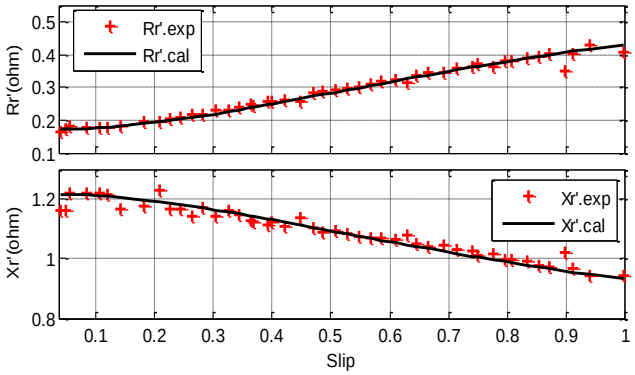

Fig.10. Variation of $R_r^{'}$ and $X_r^{'}$ in terms of slip for IM_3

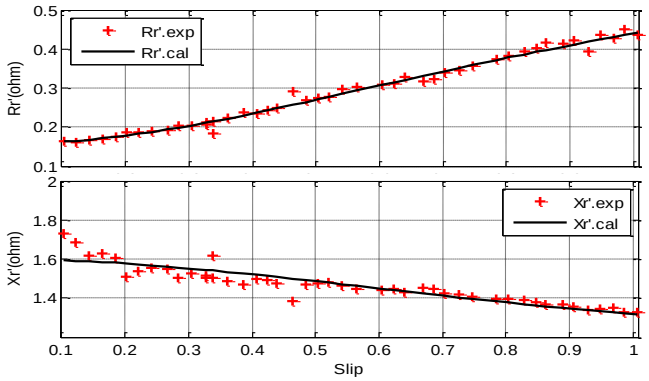

Fig.9. Variation of $R_r^{'}$ and $X_r^{'}$ in terms of slip for IM_2

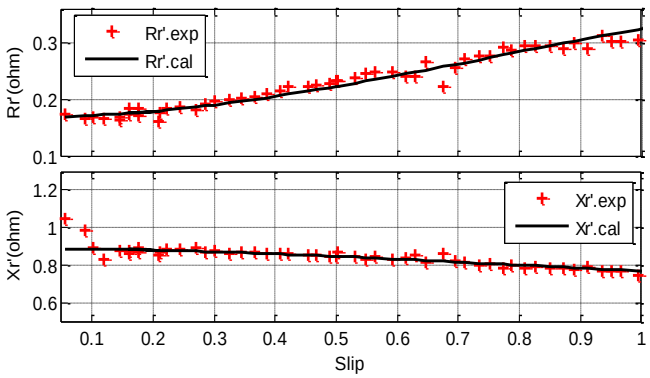

Fig.11. Variation of $R_r^{'}$ and $X_r^{'}$ in terms of slip for IM_4

IM_4 analysis gives similar *NRMSE* for models with two and three rotor branches (n = 2, 3). The leakage inductance of the third branch appears too large. It is close to L_s (cyclic inductance of the stator). For this reason the third branch is eliminated from the model and the model is considered as two branches.

Measurements of the stator current in phase *a* and the rotor speed during direct starting of IM_2 are established. The identification results of IM_2 classify it as double cage. The calculated parameters (Table 2) allows to simulate the start-up using the state model (Eq.4) for (n = 2). The measured and simulated current and speed are shown in Figures 12 and 13. A good agreement of the model and its parameters with the experimental measurements are observed. In fact, the *NRMSE*computed for the current and the speed are respectively equal to 27,26 % and 2,24%.

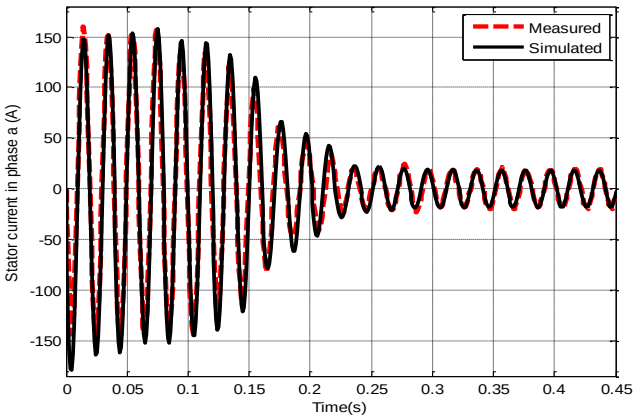

Fig.12. Comparison between simulated and measured currents in phase a for IM_2

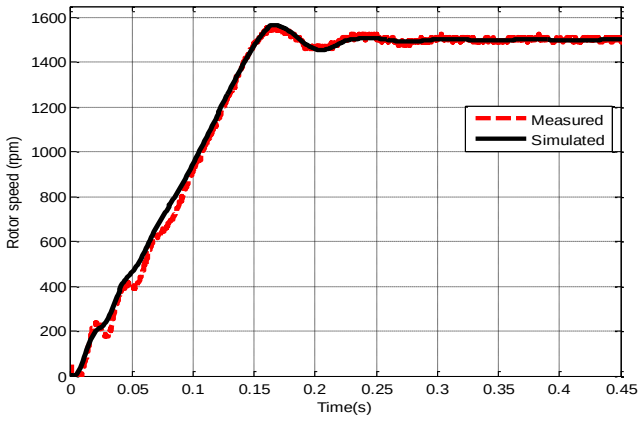

Fig.13. Comparison between simulated and measured rotor speeds for IM_2

5 Conclusion

A MIVs state model of the squirrel cage induction motor is developed. An offline IM identification based upon steady state electric measurements (voltage, stator current and active power) is elaborated by performing a locked rotor test for different frequencies. The parameters identification using the linear Least Squares Technique (LST) and the Genetic Algorithm (GA) is established. The identification and classification is validated on four IMs. The LST method is adequate as the model in the steady state is linear function of the MIVs parameters, but it shows its limitation when measurement errors increase. GA is judged more efficient since it persists and converges for a high measurement noise. The parameters that are determined by means of experimental tests are used in order to establish the dynamic model of the IM. The algorithms are verified and validated by computing *NRMSE* of measured and simulated current and speed during starting of the IM. A good agreement of model and its parameters with the experimental measurements are observed.

Nomenclature

v_{sd} , v_{sq}	dq stator voltages (V)
i_{sd} , i_{sq}	dq stator currents (A)
i_{rdi} , i_{rqi}	dq rotor currents of the ith branch (A)
V_s	phase voltage (V)
I_S	line current (A)
P	active electrical power (W)
$MIVs = [A_{h0} \quad A_{h1} \quad \dots \quad A_{hn} \quad B_{h0} \quad B_{h1} \quad \dots \quad B_{hn}]$	Invariant parameters
r_s	stator resistance (Ω)
r_i	rotor resistance of the ith branch (Ω)
L_m	mutual inductance (H)
l_i	rotor leakage inductance of the ith branch(H)
Z	input impedance of th IM per phase (Ω)
ω	synchronous angular speed (rad/s)
ω_{re}	electrical rotor speed (rad/s)
f	Synchronous frequency (Hz)
g	slip ($p.u$)
p_p	number of pairs of poles
J	total mechanical inertia ($Kg.m^2$)
C_R	load torque ($N.m$)

References

1. V.P. Sakthivel, R. Bhuvaneswari, S. Subramanian: *Artificial immune system for parameter estimation of induction motor*. In: Expert Systems with Applications, In Press, Corrected Proof, Available online 14 February 2010
2. L. Ghohdbani , F. Kourda, B. Rebhi, M. Elleuch: *Study of start up for double squirrel-cage induction motor with discret frequency control*. In: Proceedings of the 6th International Multi-Conference Systems Signals and Devices SSD '09, March 23-26, 2009, Jerba, pp 1– 7.
3. R. Babau, I. Boldea, T. J. E. Miller, N. Muntean: *Complete Parameter Identification of Large Induction Machines From No-Load Acceleration–Deceleration Tests*. In: IEEE transactions on industrial electronics, (2007) vol.54, N° 4, August 2007, pp 1962-1972.
4. R. Wamkeue, D. Aguglia, M. Lakehal, P. Viarouge: *Two-Step Method for Identification of Nonlinear Model of Induction Machine*, In: IEEE Transactions on Energy Conversion, (2007) Vol 22, December 2007 , pp 801-809.
5. D. Lindenmeyer, H. W. Dommel, A. Moshref, P. Kundur : *An induction motor parameter estimation method*. In: International Journal of Electrical Power & Energy Systems, (2001) Vol 23, Issue 4, May 2001, pp 251-262.
6. T. Lehtla. J. Joller, M. Lehtla, J. Laugis: *Parameter identification and comparision of an induction motor models*. In: Power Electronics and Variable Speed Drives, (2000) N°475, 18-19 September 2000, pp 201-205.
7. E. Levi, D. Rauski: *Modelling of deep-bar and double-cage self-excited induction generators for wind-electricity generation studies*. In: Electric Power Systems Research, (1993) Vol. 27, Issue 1, May 1993, pp 73-81.
8. W.Levy, C.F Landy, M.D McCulloch: *Improved models for the simulation of deep bar induction motors*. In: IEEE Transactions on Energy Conversion, (1990) vol5, 1990 pp 393-397.
9. P. Lund: *Induction Machine Models for Practical Use in Simulation of Transients in Power Station Auxiliaries*. In: Electric Power Systems Research, 11 (1986), 1986 pp 238 - 241
10. O. Vaag Thorsen, M. Dalva: *A comparative investigation and evaluation of different methods for experimental determination of parameters for saturated induction machines with current-displacement rotor*. In: Industry Applications Conference, 1995. Thirtieth IAS Annual Meeting, IAS '95., Conference Record of the 1995 IEEE, Vol: 1,1995 , pp 599- 605.
11. F. Córcoles, J. Pedra , M. Salichs, L. Sainz: *Analysis of the induction machine paramter identification*. In: IEEE Transactions of Energy Conversion, (2002) vol.17, June 2002, pp183-190.
12. N. Gassara, M. Chaabene, MBA Kamoun: *Smart model for the identification of the induction motor parameters*. In: Proceedings of the 6th International Multi-Conference Systems Signals and Devices SSD '09, March 23-26, 2009, Jerba, pp1 – 5, (2009) IEEE
13. A.Hamid, E. Levi, M. Raina: *A Review of RFO Induction Motor Parameter Estimation Techniques*. In: IEEE Transactions on Energy Conversion, (2003) vol.18, N°2, June 2003, pp 271.
14. Yassine Koubaa: *Asynchronous machine parameters estimation using recursive method*. In: Simulation Modelling Practice and Theory, (2006) Vol 14, Issue 7, October 2006, pp 1010-1021.
15. F. Alonge, F .D'Ippolito, F.M. Raimondi: *Least squares and genetic algorithms for parameter identification of induction motors*. In: Control Engineering Practice 9 (2001), pp 647-657.
16. Yassine Koubaa: *Recursive identification of induction motor parameters*. In: Simulation Modelling Practice and Theory, (2004) Vol 12, Issue 5, August 2004, pp 363-381.
17. J. Pedra: *On the determination of induction motor parameters from manufacturer data for electromagnetic transient programs*. In: IEEE Transactions on Energy Conversion, (2008) Vol.19,N°23, nov 2008, pp1709-1718.
18. J.Pedra: *Estimation of induction motor double-cage model parameters from manufacturer data*. In: IEEE Transactions on Energy Conversion, (2004) Vol.19,N^{o}2, June 2004, pp 310-317.
19. J. Pedra, L. Sainz: *Parameter estimation of squirrel-cage induction motors without torque measurements*. In: Electric Power Applications, IEE Proceedings, (2006) Vol 153, March 2006 , pp 263 – 270
20. A. Lima, C. Jacobina, E. Filho: *Nonlinear Parameter Estimation of Steady-State Induction Machine Models*. In: IEEE Transactions on industrial electronics, (1997), Vol. 44, N°. 3, June 1997, pp 390-397.
21. M. Çunkasa, R. Akkayab: *Design optimization of induction motor by genetic algorithm and comparison with existing motor*. In: Mathematical and Computational Applications, (2006), Vol. 11, N°. 3, pp. 193-203.
22. S Panda, S. C. Swain, A. K. Baliarsingh: *Real-coded genetic algorithm for robust coordinated design of excitation and sssc-based controller*. In: Journal of Electrical Engineering JEE, (2008), Vol. 8, 2008.
23. E. Rahimpour: *Parameter identification of deep-bar induction motors using genetic algorithm*. In: Springer-Verlag Electr Eng, (2006) vol. 89, August 2007, pp 547-552.
24. MBA. Kamoun, F. Prezezdziecki: *Frequency analysis method of variable parameter asynchronous motors*. In: Electric Machines and Power Systems, (1988) vol 15, 1988, pp 199-207.